


Systematics on the high-density nuclear equation of state from relativistic Hartree-Fock theory with Brown-Rho scaling

Si-Na Wei,^{1,*} Wei-Zhou Jiang^{2,†} and Zhao-Qing Feng^{1,‡}

¹*School of Physics and Optoelectronics, South China University of Technology, Guangzhou 510640, China*

²*School of Physics, Southeast University, Nanjing 211189, China*

 (Received 23 May 2021; revised 12 August 2021; accepted 24 September 2021; published 15 October 2021)

Using the Brown-Rho (BR) scaling law, several new relativistic Hartree-Fock (RHF) models with chiral limit are thoroughly investigated. The high-density nuclear equation of state (EOS) of RHF with the BR scaling become softer than one without the BR scaling. The EOS of RHF with BR scaling is consistent with the constraint extracted from collective flows and kaon production in heavy-ion collisions. It is found that, with a sizable strength parameter of the mass drop $x = 0.126$, the symmetry energy is almost flat at density above 3 times the saturation density ρ_0 , and even decreases slightly. This is caused from the fact that the decline of the potential part of symmetry energy is faster than the increase of the kinetic part of symmetry energy. The decrease of potential part is mainly because the neutron mass M_n^* and the proton mass M_p^* are close to each other when the density gradually approaches the critical density of chiral limit. For a mass drop of $x = 0.092$, since the critical density of chiral limit is higher than one of $x = 0.126$, the symmetry energy becomes flat at density above $5\rho_0$. While, since the critical density of chiral limit is very high for a small mass drop $x = 0.053$, the symmetry energy of RHF with $x = 0.053$ always increases at the entire density domain of this work (below $6\rho_0$). The maximum mass of neutron star (NS) obtained with present models can satisfy $M = 2.08 \pm 0.07M_\odot$. However, the radius of $1.4M_\odot$ with the mass drop of $x = 0.126$ will surpass the upper limit (13.7 km) extracted from the tidal deformability parameter of coalescence of a NS binary system and the radius of J0030+0451 being $12.71^{+1.14}_{-1.19}$ km. The radius of $1.4M_\odot$ with the mass drop of $x = 0.092$ is 13.6 km, closing to 13.7 km and the radius of J0030+0451 being $12.71^{+1.14}_{-1.19}$ km. Therefore, the RHF model with BR scaling prefers the mass drop of $x \lesssim 0.092$.

DOI: [10.1103/PhysRevC.104.045804](https://doi.org/10.1103/PhysRevC.104.045804)

I. INTRODUCTION

In-medium effects are very important in nuclear physics. It is well known that the nucleon mass will decrease to around 0.6 times at saturation density ρ_0 [1]. Experiments also show that the meson mass may decrease in the medium. The photoproduction experiments with the Crystal Barrel detector investigated in-medium modifications of the ω meson in the γ - A reactions, and reported a sizable mass drop of ω for an average density of 0.6 times saturation density [2]. The KEK proton-induced nuclear reactions also showed a sizable mass drop of ρ and ω mesons at saturation density [3]. However, the γ - A reactions with the TAPS detector indicated a small mass drop of ρ and ω mesons at saturation density [4]. Besides, in theoretical calculations, the hidden local symmetry theory showed the ρ meson becomes massless at the chiral limit [5]. The mass drop of a hadron can also be described by the scaling law established by Brown and Rho (BR) [6]. The BR scaling, which is based on an effective chiral Lagrangian of QCD, implies that hadron masses will decrease to zero at chiral limit.

Since the BR scaling is very convenient to describe the hadron mass drop and the chiral symmetry, relativistic mean-field (RMF) models with the BR scaling have been established and used to study properties of nuclear matter and a neutron star (NS), the binding energies and charge radii of finite nuclei [7–11]. However, the pion exchange, which is important in the spin-orbit interaction, is missing in the RMF. Therefore, the RMF cannot describe that the nuclear matter may undergo transitions to phases with pion condensation [12–14]. It would be interesting to introduce the BR scaling in the relativistic Hartree-Fock (RHF) approximation.

In the early days, some co-workers had tried to use RHF to study properties of nuclear matter and finite nuclei [15–18]. Due to the large incompressibility, the nuclei based on the early RHF were not bound enough, this defect being more important for light nuclei. Nowadays, there are two popular methods to obtain a reasonable incompressibility. One is to introduce the density-dependence meson-nucleon couplings into the RHF [19,20], the other is to add the nonlinear meson self-couplings into RHF [21,22]. RHF with BR scaling (RHFSL) is one kind of density-dependent RHF (DDRHF) model, but can describe chiral symmetry restoration phenomenologically. The equation of state (EOS) of theoretical models, which plays a crucial role in understanding structures of the atomic nucleus, reaction dynamics of heavy-ion

*471272396@qq.com

†wzjiang@seu.edu.cn

‡Corresponding author: fengzqh@scut.edu.cn

collisions, and properties of NSs, should be consistent with constraints extracted from the terrestrial experiments and astrophysical observations. For instance, collective flows [23] and kaon production [24–29] in heavy-ion collisions provide constraints on the EOS of symmetric nuclear matter at $1.2\text{--}4.5\rho_0$. Apart from terrestrial experiments, the mass-radius trajectories of NSs extracted from astrophysical observations have been used to constrain the EOS. The EOS should be stiff enough to support the maximum mass of NSs given by astrophysical observations. The maximum mass of NS was measured accurately through the Shapiro delay. Over the past decade, the radio pulsar J1614-2230 was found to have $M = 1.908 \pm 0.016M_\odot$ [30–32], and the J0348+0432 was found to have $M = 2.01 \pm 0.04M_\odot$ [33]. The mass of millisecond pulsar J0740+6620 was measured to be $M = 2.14^{+0.10}_{-0.09}M_\odot$ with 68.3% confidence and $M = 2.14^{+0.20}_{-0.18}M_\odot$ with 95.4% confidence [34]. Now, the mass of J0740+6620 has been updated to be $M = 2.08 \pm 0.07M_\odot$ with 68.3% confidence [35]. Unfortunately, the radius of NS, which is extracted from astrophysical observations, still has a large uncertainty suffered from the distance measurements and theoretical analyses of the light spectrum. In the past, the radius of NS with $1.4M_\odot$ extracted from optical observations ranged roughly 10–14 km [36–42]. More recently, the Neutron Star Interior Composition Explorer (NICER) collaboration used a Bayesian inference approach to analyze energy-dependent thermal x-ray waveform of millisecond pulsar J0030+0451, and found that the radius (mass) of J0030+0451 is $13.02^{+1.24}_{-1.06}$ km ($M = 1.44^{+0.15}_{-0.14}M_\odot$) [43] or $12.71^{+1.14}_{-1.19}$ km ($M = 1.34^{+0.15}_{-0.16}M_\odot$) [44]. Apart from optical measurement, an alternative way to extract the radius of NSs is based on the gravitational-wave signals of NS mergers. Based on the tidal deformability parameter of the coalescence of a NS binary system, the radius of NS with $1.4M_\odot$ was predicted to have an upper limit which is about 13.7 km [45–49]. The radius range of NS with $1.4M_\odot$ implies that the EOS should be soft below the central density of $1.4M_\odot$.

This work is arranged as follows. In Sec. II, the formalism for obtaining the EOS of RHF theory with BR scaling is briefly introduced. The numerical results and discussions including properties of nuclear matter and NS are presented in Sec. III. Finally, a brief summary is given.

II. FORMALISM

The Lagrangian density for hadron is written as follows [15–22]:

$$\mathcal{L} = \mathcal{L}_0 + \mathcal{L}_I, \quad (1)$$

where \mathcal{L}_0 and \mathcal{L}_I are the free Lagrangian density and the interaction Lagrangian density, respectively,

$$\begin{aligned} \mathcal{L}_0 = & \sum_B \bar{\psi}_B (i\gamma_\mu \partial^\mu - M_B) \psi_B + \frac{1}{2} (\partial_\mu \sigma \partial^\mu \sigma - m_\sigma^{*2} \sigma^2) \\ & + \frac{1}{2} m_\omega^{*2} \omega_\mu \omega^\mu - \frac{1}{4} F_{\mu\nu} F^{\mu\nu} + \frac{1}{2} m_\rho^{*2} \rho_\mu \cdot \rho^\mu \\ & - \frac{1}{4} \mathbf{G}_{\mu\nu} \cdot \mathbf{G}^{\mu\nu} + \frac{1}{2} (\partial_\mu \boldsymbol{\pi} \partial^\mu \boldsymbol{\pi} - m_\pi^{*2} \boldsymbol{\pi}^2), \end{aligned} \quad (2)$$

ψ_B and M_B are the baryon field and the rest mass of baryon. σ , ω , ρ , and $\boldsymbol{\pi}$ are the meson field, and m_σ^* , m_ω^* , m_ρ^* , and m_π^* are the corresponding scaled mass in the medium. $F_{\mu\nu}$ and $\mathbf{G}_{\mu\nu}$ are the field strength tensors of ω and ρ mesons, and expressed as follows:

$$F_{\mu\nu} = \partial_\nu \omega_\mu - \partial_\mu \omega_\nu, \quad \mathbf{G}_{\mu\nu} = \partial_\nu \boldsymbol{\rho}_\mu - \partial_\mu \boldsymbol{\rho}_\nu. \quad (3)$$

The interaction Lagrangian density means the interaction between nucleons is achieved by exchanging a meson. In the current work, since we do not consider isoscalar- and isovector-tensor coupling, there are only four expressions lived:

$$\begin{aligned} \mathcal{L}_I = & -g_\sigma^* \bar{\psi} \sigma \psi - g_\omega^* \bar{\psi} \gamma_\mu \omega^\mu \psi - g_\rho^* \bar{\psi} \gamma_\mu \boldsymbol{\rho}^\mu \cdot \boldsymbol{\tau} \psi \\ & - \frac{f_\pi^*}{m_\pi^*} \bar{\psi} \gamma_5 \boldsymbol{\gamma}_\mu \partial^\mu \boldsymbol{\pi} \cdot \boldsymbol{\tau} \psi, \end{aligned} \quad (4)$$

where the $\boldsymbol{\tau}$ is isospin Pauli matrix. g_σ^* , g_ω^* , g_ρ^* , and f_π^* are the scaled meson-nucleon coupling constants in the medium.

Neglecting the small Coulomb field in infinite nuclear matter, with the time-reversal symmetry and rotational invariance, the self-energy of baryon Σ_B can be expanded as follows:

$$\Sigma_B(k) = \Sigma_B^S(k) + \gamma_0 \Sigma_B^0(k) + \boldsymbol{\gamma} \cdot \hat{\mathbf{k}} \Sigma_B^V(k), \quad (5)$$

where $\hat{\mathbf{k}}$ is the unit vector along \mathbf{k} . Σ_B^S , Σ_B^0 , and Σ_B^V are the scalar, time, and space components of the self-energy, respectively. With the self-energy, the effective nucleon mass, momentum, and energy are defined as

$$\begin{aligned} M_B^*(k) &= M_B + \Sigma_B^S(k), \\ \mathbf{k}^* &= \mathbf{k} + \hat{\mathbf{k}} \Sigma_B^V(k), \\ E_B^*(k) &= \sqrt{M_B^{*2} + \mathbf{k}^{*2}}. \end{aligned} \quad (6)$$

For further simplicity, we write $\hat{K} \equiv \frac{\mathbf{k}^*}{E_B^*}$ and $\hat{M}_B \equiv \frac{M_B^*}{E_B^*}$. By taking the ground state expectation of the Hamiltonian ($H = T + V_D + V_E$), the energy density includes the baryon and meson contributions can be written as [18,20]

$$\begin{aligned} \epsilon &= \epsilon_K + \epsilon_D + \epsilon_E, \quad (7) \\ \epsilon_K &= \sum_{B=n,p} \frac{1}{\pi^2} \int_0^{k_{F,B}} k^2 dk (k \hat{K} + M_B \hat{M}_B), \\ \epsilon_D &= -\frac{1}{2} \frac{g_\sigma^{*2}}{m_\sigma^{*2}} \rho_s^2 + \frac{1}{2} \frac{g_\omega^{*2}}{m_\omega^{*2}} \rho^2 + \frac{1}{2} \frac{g_\rho^{*2}}{m_\rho^{*2}} \rho_3^2, \\ \epsilon_E &= \frac{1}{2} \frac{1}{(2\pi)^4} \sum_{\alpha, B, B'} \int_0^{k_{F,B}} \int_0^{k_{F,B'}} k k' dk dk' \\ & \times \{ \delta_{BB'} [A_\alpha(k, k') + \hat{M}_B(k) \hat{M}_{B'}(k') B_\alpha(k, k') \\ & + \hat{K}(k) \hat{K}(k') C_\alpha(k, k')]_{\sigma, \omega} + (2 - \delta_{BB'}) [A_\alpha(k, k') \\ & + \hat{M}_B(k) \hat{M}_{B'}(k') B_\alpha(k, k') \\ & + \hat{K}(k) \hat{K}(k') C_\alpha(k, k')]_{\rho, \pi} \}. \end{aligned} \quad (8)$$

k_F is the Fermi momentum. ρ , ρ_s , and ρ_3 are the baryon density, the scalar density, and the third component of isovector density. ϵ_K , ϵ_D , and ϵ_E are the kinetic energy density, the

TABLE I. The functions A_α , B_α , and C_α in Eqs. (11) and (8).

α	$A_\alpha(k, k')$	$B_\alpha(k, k')$	$C_\alpha(k, k')$
σ	$g_\sigma^{*2} \Theta_\sigma(k, k')$	$g_\sigma^{*2} \Theta_\sigma(k, k')$	$-2g_\sigma^{*2} \Phi_\sigma(k, k')$
ω	$2g_\omega^{*2} \Theta_\omega(k, k')$	$-4g_\omega^{*2} \Theta_\omega(k, k')$	$-4g_\omega^{*2} \Phi_\omega(k, k')$
ρ	$2g_\rho^{*2} \Theta_\rho(k, k')$	$-4g_\rho^{*2} \Theta_\rho(k, k')$	$-4g_\rho^{*2} \Phi_\rho(k, k')$
π	$-f_\pi^{*2} \Theta_\pi(k, k')$	$-f_\pi^{*2} \Theta_\pi(k, k')$	$2 \frac{f_\pi^{*2}}{m_\pi^{*2}} [(k^2 + k'^2) \Phi_\pi(k, k') - kk' \Theta_\pi(k, k')]$

direct, and exchange terms of the potential energy density, respectively. $\delta_{BB'}$ and $2 - \delta_{BB'}$ are the isospin factor for isoscalar and isovector, respectively. The α runs over σ and ω (ρ and π) mesons. The functions A_α , B_α , and C_α are given in Table I, with the following functions:

$$\Theta_\alpha(k, k') = \ln \left[\frac{m_\alpha^{*2} + (k + k')^2}{m_\alpha^{*2} + (k - k')^2} \right],$$

$$\Phi_\alpha(k, k') = \frac{1}{4kk'} (k^2 + k'^2 + m_\alpha^{*2}) \Theta_\alpha(k, k') - 1. \quad (9)$$

For simplicity, in this work, we use a numerical calculation to solve the pressure P , the incompressibility κ , the symmetry energy E_{sym} , and the slope of symmetry energy L :

$$P = \rho^2 \frac{\partial(\epsilon/\rho)}{\partial\rho},$$

$$\kappa = \rho \frac{d^2\epsilon}{d\rho^2} = 9 \frac{dP}{d\rho},$$

$$E_{\text{sym}}(\rho) = \frac{1}{2} \frac{\partial^2(\epsilon/\rho)}{\partial\delta^2} \Big|_{\delta=0},$$

$$L = 3\rho_0 \frac{\partial E_{\text{sym}}(\rho)}{\partial\rho} \Big|_{\rho_0} \quad (10)$$

with ρ_0 being the saturation density. $\delta = (\rho_n - \rho_p)/\rho$ is the isospin asymmetry parameter.

By differentiating the potential energy densities (ϵ_D and ϵ_E) of Eq. (8) with respect to the Dirac spinor, the scalar, time, and space components of the self-energy are given as [18,20]

$$\Sigma_B^S(k) = -\frac{g_\sigma^{*2}}{m_\sigma^{*2}} \rho_S + \frac{1}{(4\pi)^2 k} \sum_{\alpha, B'} \int_0^{k_{F, B'}} k' dk' \hat{M}_B(k')$$

$$\times [\delta_{BB'} B_\alpha(k, k')_{\sigma, \omega} + (2 - \delta_{BB'}) B_\alpha(k, k')_{\rho, \pi}],$$

$$\Sigma_B^0(k) = \frac{g_\omega^{*2}}{m_\omega^{*2}} \rho + \frac{1}{(4\pi)^2 k} \sum_{\alpha, B'} \int_0^{k_{F, B'}} k' dk'$$

$$\times [\delta_{BB'} A_\alpha(k, k')_{\sigma, \omega} + (2 - \delta_{BB'}) A_\alpha(k, k')_{\rho, \pi}],$$

$$\Sigma_B^V(k) = \frac{1}{(4\pi)^2 k} \sum_{\alpha, B'} \int_0^{k_{F, B'}} \hat{K}(k') k' dk'$$

$$\times [\delta_{BB'} C_\alpha(k, k')_{\sigma, \omega} + (2 - \delta_{BB'}) C_\alpha(k, k')_{\rho, \pi}]. \quad (11)$$

Equations (6) and (11) can be solved with a self-consistent calculation. And then, the energy density, the pressure, the incompressibility, the symmetry energy, and the slope of symmetry energy are easy to work out.

The innovation of this work is that we consider the BR scaling in RHF. Similar to the SLC and SLCD models which

can successfully describe the properties of NS and finite nuclei [10,11], we ignore the BR scaling for the nucleon mass M_B . For mesons' mass, the BR scaling functions are introduced as [2,3,6,9–11]

$$\frac{m_\sigma^*}{m_\sigma} = \frac{m_\omega^*}{m_\omega} = \frac{m_\rho^*}{m_\rho} = \frac{f_\pi^*}{f_\pi} = 1 - x \frac{\rho}{\rho_0}, \quad (12)$$

where x is the strength parameter of the mass drop. Different from Eq. (12), the pion mass m_π^* , which is missing in the RMF, scales as $\sqrt{f_\pi^*}$ [6]. Apart from f_π^* , the scaling functions of coupling constants are given as [10,11]

$$\frac{g_\sigma^*}{g_\sigma} = \frac{1}{1 + y\rho/\rho_0},$$

$$\frac{g_\omega^*}{g_\omega} = \frac{1 - x\rho/\rho_0}{1 + w\rho/\rho_0}, \quad (13)$$

$$\frac{g_\rho^*}{g_\rho} = \frac{1 - x\rho/\rho_0}{1 + z\rho/\rho_0}.$$

The strength parameter of the mass drop x is given based on the experimental results. When x is given, the remaining scaling parameters of coupling constants y and z are chosen to adjust the incompressibility κ and the slop of symmetry energy, respectively. The scaling parameter w will stiffen the EOS at low density and soften the EOS at high density, so that the properties of finite nuclei and NS are not very reasonable. In the following, similar to the SLC and SLCD models, we set w to be zero.

III. RESULTS AND DISCUSSIONS

The EOS of earlier RMF and RHF is quite stiff [17,50]. In order to soften the EOS, nonlinear meson self-interactions and density-dependence meson-nucleon couplings are introduced in the RMF and RHF [7–11,21–24,51]. As one kind of density-dependence model, RMF with the BR scaling can produce a soft EOS and describe chiral symmetry restoration phenomenologically [7–11]. The RMF with BR scaling has been established to study properties of NS and finite nuclei successfully. However, the pion exchange, which is important in the spin-orbit interaction, is missing in the RMF. In order to take into account the contributions of pion exchange in the nucleon-nucleon force, we have established several RHF with BR scaling.

The strength parameter of the mass drop x is given based on the experimental results. The photoproduction experiments with the Crystal Barrel detector reported a sizable mass drop $x \approx 0.13$ of ω for an average density of 0.6 times saturation density [2]. The KEK proton-induced nuclear reactions also reported a sizable mass drop $x = 0.092 \pm 0.002$ of ρ and ω

TABLE II. Parameter sets for RMF and RHF models. The hadron masses are $M_B = 938$ MeV, $m_\sigma = 590$ MeV, $m_\omega = 783$ MeV, $m_\rho = 770$ MeV, and $m_\pi = 138$ MeV in vacuum. E_B/A (MeV), κ (MeV), E_{sym} (MeV), and L (MeV) are the binding energy, incompressibility, symmetry energy, and slope of symmetry energy at saturation density $\rho_0 = 0.16$ fm $^{-3}$, respectively. The radius R is in units of km.

Model	g_σ	g_ω	g_ρ	f_π	x	y	z	E_B/A (MeV)	κ (MeV)	E_{sym} (MeV)	L (MeV)	M_{max}/M_\odot	$R(1.4M_\odot)$
SLC	10.1408	10.3261	3.8021	—	0.126	0.239	—	−16.3	230.0	31.6	92.3	2.01	12.6
SLCD	10.1408	10.3261	5.7758	—	0.126	0.239	0.5191	−16.3	230.0	31.6	61.5	2.00	11.5
RHFSL1	10.410	10.190	1.721	—	0.126	0.239	—	−16.0	300.6	31.6	90.4	1.84	13.6
RHFSLD1	10.236	9.978	2.832	—	0.126	0.239	0.5191	−16.0	276.3	31.6	79.7	1.74	13.2
RHFSLD2	9.863	9.798	2.468	1.000	0.126	0.239	0.5191	−16.0	237.8	31.6	76.9	1.71	12.5
RHFSLD3	10.485	10.838	0.130	1.000	0.126	0.210	0.5191	−16.0	301.0	31.6	96.0	2.06	13.9
RHFSLD4	9.898	10.063	1.905	1.000	0.092	0.170	0.5191	−16.0	303.8	31.6	84.7	2.13	13.6
RHFSLD5	9.148	8.922	2.789	1.000	0.053	0.140	0.5191	−16.0	292.3	31.6	73.1	2.09	13.1
RHF	10.607	11.759	—	1.000	—	—	—	−16.0	524.7	37.9	149.2	2.80	15.0

meson at saturation density [3]. However, the γ - A reactions with the TAPS detector concluded that the mass drop x is not greater than 0.053 for ρ and ω mesons at saturation density [4]. The mass drop of SLC and SLCD is based on the result of the photoproduction experiments with the Crystal Barrel detector [10,11]. As shown in Table II, for comparison, we first choose the same BR scaling parameters as the SLC and SLCD in RHFSL1 and RHFSLD1, respectively, and ignore the pion's contributions. When the BR scaling parameters (x, y, w) are set, the meson-nucleon coupling constants ($g_\sigma, g_\omega, g_\rho$) are adjusted to reproduce the binding energy per nucleon $E_B/A = \epsilon/\rho - M_B = -16.0$ MeV, the zero pressure and the average value of symmetry energy $E_{\text{sym}} = 31.6$ MeV at saturation density $\rho_0 = 0.16$ fm $^{-3}$ [52]. Since the ρ meson has no contributions in symmetric nuclear matter with RMF, the EOS of symmetric nuclear matter between SLC and SLCD has no differences. The SLC and SLCD models share the same incompressibility $\kappa = 230$ MeV at saturation density. However, since the ρ meson has contributions in the Fock term of symmetric nuclear matter, the EOS of symmetric nuclear matter between RHFSL1 and RHFSLD1 is different. The EOS of RHFSLD1, which considers the BR scaling parameter of the coupling constant of ρ meson z , is softer than one of RHFSL1. Due to the contributions of the Fock term, with the same BR scaling parameters, the EOS of RHF is stiffer than the one of RMF. When the contributions of the pion are taken into account and the rest of the BR scaling parameters remain the same, the EOS of RHF will become soft. For instance, the EOS of RHFSLD2 is much softer than the one of RHFSLD1. Such a soft EOS may not be conducive to reproducing the properties of NSs. Therefore, for a given mass drop x , we reduce the BR scaling parameter y of the coupling constant of the σ meson to stiffen the EOS of RHF. As shown in Table II, keeping the rest of the BR scaling parameters unchanged, the incompressibility increases with a decreasing of the BR scaling parameter y . Moreover, since the size of the mass drop remains controversial [53], we also study the RHF with the mass drop of $x = 0.092$ [3] and $x = 0.053$ [4]. The EOS of RHF without BR scaling is also listed for comparison.

When the RHF models with BR scaling are established, we are interested in how these models reflect the chiral limit. The corresponding critical density ρ_c of the chiral symmetry restoration with a mass drop $x = 0.126$, $x = 0.092$, and

$x = 0.053$ is 7.94, 10.87, and 18.87 ρ_0 , respectively. As shown in Fig. 1, for a given mass drop x , the nucleon mass of RHF models becomes zero at the same density. The nucleon mass of RHF models with $x = 0.126$ approaches zero the fastest. A zero mass of a nucleon will not break the chiral symmetry. Due to the Fock term, the nucleon mass of RHF will reach zero faster than one of the RMFs with the same strength parameter of the mass drop. The RHF without BR scaling will not reach zero at high density. Moreover, as shown in Fig. 2, we compare the pressures of BR scaling models with constraints from collective flows [23] and kaon production [24–29] in heavy-ion collisions. The pressures of RHF with BR scaling are consistent with the constraints from collective flows and kaon production. For a sizable mass drop $x = 0.126$, since RHF with BR scaling reach the chiral limit quickly, the pressures of these models will rise up at 5–6 ρ_0 . While, for the mass drop of $x = 0.092$ and $x = 0.053$, the pressures will not rise up at 5–6 ρ_0 . Besides, a small scaling parameter of scalar coupling constant y will lead to a larger incompressibility and a higher pressure. For a given mass drop x , the pressures of RHF with BR scaling can almost range from the lowest constraint to the highest constraint by varying scaling parameters of scalar coupling constant y . This will be helpful for us to

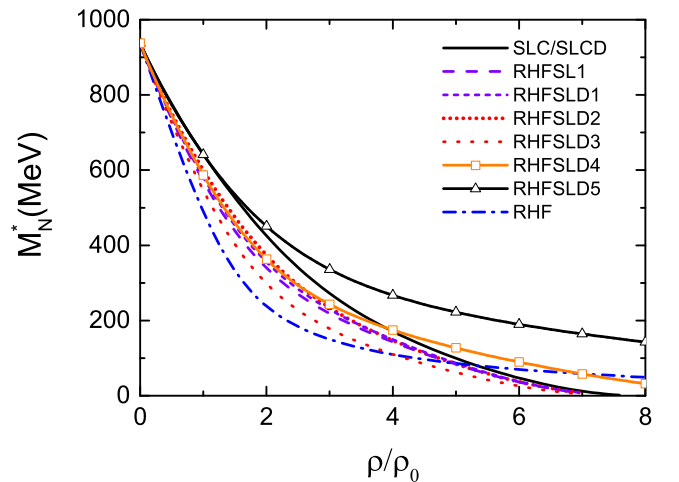


FIG. 1. The effective mass as a function of baryon density in symmetric nuclear matter for RHF with different parameters.

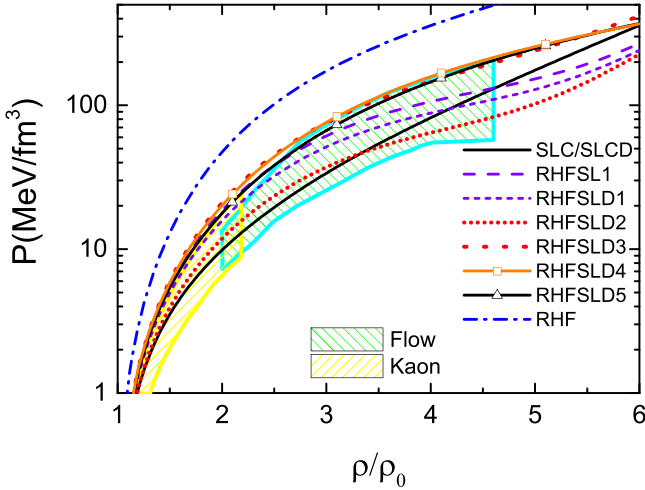


FIG. 2. The pressure as a function of baryon density in symmetric nuclear matter for RHF with different parameters. The cyan and yellow regions extracted from the collective flows [23] and kaon [24–29] yields of heavy-ion collisions, respectively.

study the properties of NS. Since the EOS of the RHF without BR scaling is rather stiff, the pressure of this model surpasses the constraint obviously.

The symmetry energy, which is the energy difference per nucleon between pure neutron matter and symmetric matter, is also an important part of EOS. Apart from the RHF model without BR scaling, as shown in Table II and Fig. 3, the symmetry energy is set to an average value (31.6 MeV) at saturation density. The symmetry energy of the RHF model without BR scaling is stiff. However, when considering the BR scaling, the symmetry energy of the RHF model becomes soft. The slope of symmetry energy of RHF with BR scaling ranges from 73.1 MeV to 96.0 MeV. Although some of the slopes of symmetry energy are higher than the average slope of the symmetry energy of 59.8 ± 16.5 MeV [53], however, values beyond this average domain still cannot be excluded. Some extractions of experimental/observational data still support a higher slope of symmetry energy. For instance, the slopes of symmetry energy extracted from isospin diffusion at 50 MeV/A with IBUU04 and IQMD are 86 ± 25 MeV [54] and 77.5 ± 32.5 MeV [55], respectively. The slopes of symmetry energy extracted from charge exchange and elastic scattering reactions is about 70–101 MeV [56]. More recently, the slope of symmetry energy, which is extracted from spectra of charged pions in collisions involving rare isotope Sn beams on isotopic Sn targets, ranges from 42 to 117 MeV [57]. The slope of symmetry energy extracted from the recent neutron skin thickness of ^{208}Pb given by the PREX-II is 109.56 ± 36.41 MeV [58]. Also, the slopes of symmetry energy extracted from torsional crust oscillation of NSs is 115 ± 15 MeV [59]. Interestingly, as shown in the upper panel of Fig. 3, the symmetry energy of RHF with the strength parameter of the mass drop $x = 0.126$ (RHFSL1-RHFSLD3) is almost flat at density above $3\rho_0$, and even decreases slightly. To explain this phenomenon, we decompose the symmetry energy into a kinetic part $E_{\text{sym}}^{\text{kin}} = \frac{1}{2} \frac{\partial^2(\epsilon_K/\rho)}{\partial \delta^2} |_{\delta=0}$ and potential part $E_{\text{sym}}^{\text{pot}} = \frac{1}{2} \frac{\partial^2((\epsilon_D + \epsilon_E)/\rho)}{\partial \delta^2} |_{\delta=0}$ [60]. As shown in lower panel

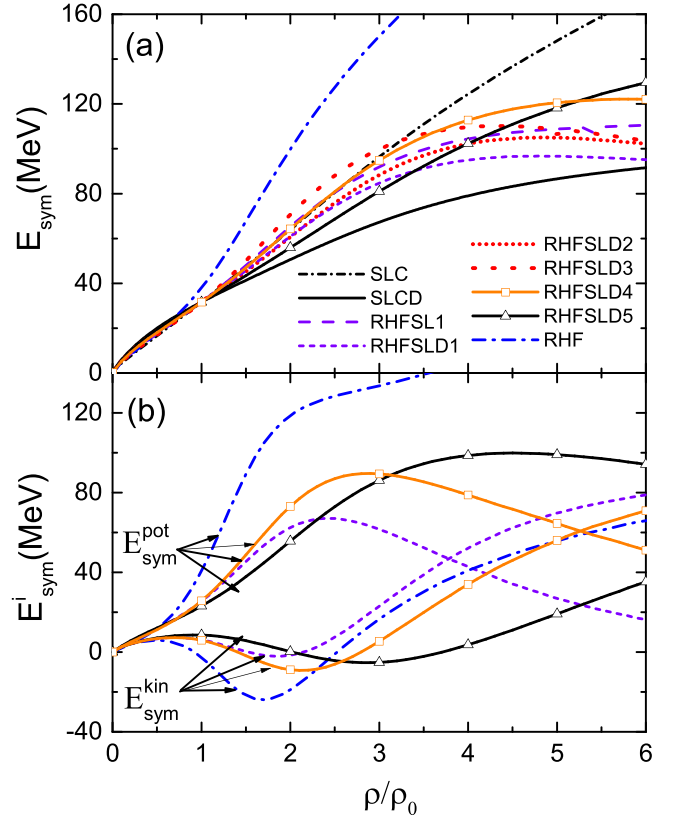


FIG. 3. The symmetry energy as a function of baryon density for RHF with different parameters (upper panel). The lower panel is the kinetic and potential parts of the symmetry energy as a function of baryon density.

of Fig. 3, for $x = 0.126$, the kinetic part of the symmetry energy increases at a density above $3\rho_0$, however, the potential part of the symmetry energy decreases. When the potential part decreases faster than the kinetic part is increasing, the symmetry energy will decrease slightly. The decrease of the potential part is mainly because the neutron mass M_n^* and the proton mass M_p^* are close to each other when the density gradually approaches the critical density of chiral limit. For $x = 0.092$ (RHFSLD4), since the critical density of the chiral limit is higher than the one of $x = 0.126$, the symmetry energy becomes flat at a density above $5\rho_0$. For $x = 0.053$ (RHFSLD5), the difference between M_n^* and M_p^* remains at a density below $6\rho_0$. As a result, the potential part with $x = 0.053$ will hardly drop and the symmetry energy increases with an increase of the baryon density at a density below $6\rho_0$. Similarly, the potential part of RHF without BR scaling does not decrease [60]. After discussing the EOS of RHF with BR scaling, we turn to investigate the properties of NSs. We consider that the matter of NS consists of neutrons, protons, electrons, and muons. With the β equilibrium conditions ($\mu_p = \mu_n - \mu_e$, $\mu_\mu = \mu_e$) and charge neutrality ($\rho_p = \rho_e + \rho_\mu$), the density of each component of NS matter is determined. Then the energy density ($\epsilon_{ns} = \epsilon + \epsilon_\mu + \epsilon_e$) and the pressure P of NS matter can be obtained. We adopt the EOSs obtained in this work at densities above half the saturation density, while we employ the standard low-density

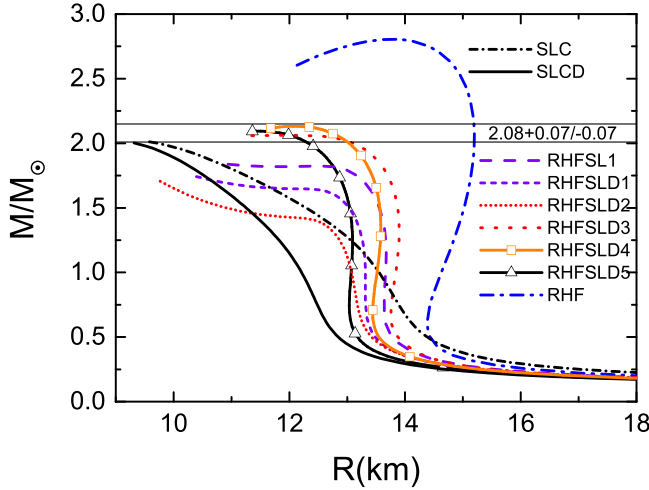


FIG. 4. The mass-radius trajectories of NSs for RHF with different parameters.

EOS since at lower densities NS matter transitions to the inhomogeneous phase [61,62]. With the energy density and pressure as inputs, the NS mass-radius relation can be obtained by solving the standard Tolman-Oppenheimer-Volkoff (TOV) equation [63,64]. As shown in Fig. 4, with the same BR scaling parameters as the SLC and SLCD, the RHFSL1 and RHFSLD1, which do not contain the contributions of a pion, can support the NS maximum mass of $1.84 M_{\odot}$ and $1.74 M_{\odot}$, respectively. When including the pion and taking the rest BR scaling parameters as RHFSLD1, the NS maximum mass given by the RHFSLD2 is merely $1.71 M_{\odot}$. The maximum mass of the RHFSL1, RHFSLD1, and RHFSLD2 does not satisfy the recent astrophysical measurement ($M = 2.08 \pm 0.07 M_{\odot}$ [35]). In order to satisfy this measurement, we reduce the BR scaling parameter of scalar coupling constant y to stiffen the EOS. As a consequence, the NS maximum mass predicted by RHFSLD3 is $M = 2.06 M_{\odot}$, and is well within the domain of the recent astrophysical measurement. For the mass drop of $x = 0.092$ and $x = 0.053$, RHF with BR scaling can also be adjusted to satisfy the maximum mass extracted from recent astrophysical measurement. Apart from the maximum mass, the radius of $M = 2.08 \pm 0.07 M_{\odot}$ predicted by RHFSLD3-RHFSLD5 is consistent with the results extracted from astrophysical observations ($12.39^{+1.30}_{-0.98}$ km [65] or $13.7^{+2.6}_{-1.5}$ km [66]). Moreover, the radius of $1.4 M_{\odot}$ predicted by RHFSLD3-RHFSLD5 ranges from 13.1 to 13.9 km, locating at extractions from optical observations ranging roughly from 10 to 14 km [36–42] and the radius of J0030+0451 being $13.02^{+1.24}_{-1.06}$ km [43]. However, the radius of $1.4 M_{\odot}$ with RHFSLD3 surpasses the upper limit (13.7 km) based on the tidal deformability parameter of coalescence of a NS binary system [45–49] and the radius of J0030+0451 being $12.71^{+1.14}_{-1.19}$ km [44]. For a given mass drop $x = 0.126$, although we can adjust the scaling parameter y of RHF to obtain

the maximum mass in the $M = 2.08 \pm 0.07 M_{\odot}$ domain, the radius of $1.4 M_{\odot}$ will surpass the upper limit based on the tidal deformability parameter of the coalescence of a NS binary system and the radius of J0030+0451 being $12.71^{+1.14}_{-1.19}$ km. The NS radius of $1.4 M_{\odot}$ with $x = 0.092$ is 13.6 km, closing to the upper limit based on the tidal deformability parameter of a coalescence of a NS binary system and the radius of J0030+0451 being $12.71^{+1.14}_{-1.19}$ km. As a conclusion, the mass drop of the RHF model cannot be too sizable, i.e., it shall not exceed $x = 0.092$.

IV. SUMMARY

In this work, due to the chiral symmetry restoration at high densities, several RHF with various mass drops of mesons have been proposed. Since the controversy about the size of the mass drop of mesons still remains, the mass drops of RHF are chosen as $x = 0.126$, $x = 0.092$, and $x = 0.053$ based on the experimental results. The pressure of symmetric nuclear matter with these new models is consistent with the constraint extracted from collective flows and kaon production in heavy-ion collisions. Interestingly, the symmetry energy of RHF with BR scaling becomes soft at high density. Moreover, with a sizable mass drop $x = 0.126$, the symmetry energy is almost flat at densities above $3\rho_0$, and even decreases slightly. This is because the potential part of the symmetry energy decreases at density above $3\rho_0$. The decrease of the potential part is caused from the fact that the neutron mass M_n^* and the proton mass M_p^* are close to each other when the density gradually approaches the critical density of chiral limit. With a mass drop of $x = 0.092$, since the critical density of the chiral limit is higher than the one of $x = 0.126$, the symmetry energy becomes flat at densities above $5\rho_0$. For a small mass drop $x = 0.053$, since the critical density of the chiral limit is very high, the potential part of symmetry energy hardly decreases at densities below $6\rho_0$. Therefore, the symmetry energy of RHF with $x = 0.053$ always increases at densities below $6\rho_0$. Using RHF with BR scaling, we also investigated the NS mass-radius relations. Apart from three soft EOSs (RHFSL1, RHFSLD1, and RHFSLD2), the NS maximum mass obtained from RHF with BR scaling satisfies $M = 2.08 \pm 0.07 M_{\odot}$. However, the NS radius of $1.4 M_{\odot}$ with a sizable mass drop $x = 0.126$ will surpass the upper limit (13.7 km) based on the tidal deformability parameter of the coalescence of a NS binary system and the radius of J0030+0451 being $12.71^{+1.14}_{-1.19}$ km. The NS radius of $1.4 M_{\odot}$ with $x = 0.092$ is 13.6 km, closing to 13.7 km, and the radius of J0030+0451 being $12.71^{+1.14}_{-1.19}$ km. As a conclusion, the mass drop of RHF model shall not exceed $x = 0.092$.

ACKNOWLEDGMENT

The work was supported by the National Natural Science Foundation of China under Grants No. 11722546, No. 12175072, and No. 11775049.

[1] R. J. Furnstahl, X. Jin, and D. B. Leinweber, *Phys. Lett. B* **387**, 253 (1996).

[2] D. Trnka, G. Anton, J. C. S. Bacelar, O. Bartholomy *et al.*, *Phys. Rev. Lett.* **94**, 192303 (2005).

- [3] M. Naruki, Y. Fukao, H. Funahashi, M. Ishino, H. Kanda, M. Kitaguchi, S. Mihara, K. Miwa, T. Miyashita, T. Murakami, T. Nakura, F. Sakuma, M. Togawa, S. Yamada, Y. Yoshimura, H. Enyo, R. Muto, T. Tabaru, S. Yokkaichi, J. Chiba, M. Ieiri, O. Sasaki, M. Sekimoto, K. H. Tanaka, H. Hamagaki, and K. Ozawa, *Phys. Rev. Lett.* **96**, 092301 (2006).
- [4] M. H. Wood, R. Nasseripour, D. P. Weygand, C. Djalali *et al.*, *Phys. Rev. C* **78**, 015201 (2008).
- [5] M. Harada and K. Yamawaki, *Phys. Rep.* **381**, 1 (2003).
- [6] G. E. Brown and M. Rho, *Phys. Rev. Lett.* **66**, 2720 (1991).
- [7] C. Song, *Phys. Rep.* **347**, 289 (2001).
- [8] B. Liu, H. Guo, V. Greco *et al.*, *Eur. Phys. J. A* **22**, 337 (2004).
- [9] S. S. Avancini and D. P. Menezes, *Phys. Rev. C* **74**, 015201 (2006).
- [10] W. Z. Jiang, B. A. Li, and L. W. Chen, *Phys. Lett. B* **653**, 184 (2007).
- [11] W. Z. Jiang, B. A. Li, and L. W. Chen, *Phys. Rev. C* **76**, 054314 (2007).
- [12] A. B. Migdal, *Rev. Mod. Phys.* **50**, 107 (1978).
- [13] A. Akmal, V. R. Pandharipande, and D. G. Ravenhall, *Phys. Rev. C* **58**, 1804 (1998).
- [14] D. B. Kaplan, and A. E. Nelson, *Phys. Lett. B* **175**, 57 (1986).
- [15] M. Jaminon, C. Mahaux, and P. Rochus, *Nucl. Phys. A* **365**, 371 (1981).
- [16] C. J. Horowitz, and B. D. Serot, *Nucl. Phys. A* **399**, 529 (1983).
- [17] A. Bouyssy, S. Marcos, J. F. Mathiot, and N. Van Giai, *Phys. Rev. Lett.* **55**, 1731 (1985).
- [18] A. Bouyssy, J. F. Mathiot, N. Van Giai, and S. Marcos, *Phys. Rev. C* **36**, 380 (1987).
- [19] W. H. Long, H. Sagawa, N. V. Giai, and J. Meng, *Phys. Rev. C* **76**, 034314 (2007).
- [20] B. Y. Sun, W. H. Long, J. Meng, and U. Lombardo, *Phys. Rev. C* **78**, 065805 (2008).
- [21] P. Bernardos, V. N. Fomenko, N. V. Giai, M. L. Quelle, S. Marcos, R. Niembro, and L. N. Savushkin, *Phys. Rev. C* **48**, 2665 (1993).
- [22] T. Miyatsu, T. Katayama, and K. Saito, *Phys. Lett. B* **709**, 242 (2012).
- [23] P. Danielewicz, R. Lacey, and W. G. Lynch, *Science* **298**, 1592 (2002).
- [24] W. G. Lynch, M. B. Tsang, Y. Zhang, P. Danielewicz, M. Famiano, Z. Li, and A. W. Steiner, *Prog. Part. Nucl. Phys.* **62**, 427 (2009).
- [25] I. Sagert, L. Tolos, D. Chatterjee, J. Schaffner-Bielich, and C. Sturm, *Phys. Rev. C* **86**, 045802 (2012).
- [26] C. Fuchs, A. Faessler, E. Zabrodin, and Y. M. Zheng, *Phys. Rev. Lett.* **86**, 1974 (2001).
- [27] C. Hartnack, H. Oeschler, and J. Aichelin, *Phys. Rev. Lett.* **96**, 012302 (2006).
- [28] G. Ferini, T. Gaitanos, and M. Colonna, M. DiToro, and H. H. Wolter, *Phys. Rev. Lett.* **97**, 202301 (2006).
- [29] Z. Q. Feng, *Phys. Rev. C* **83**, 067604 (2011).
- [30] P. Demorest, T. Pennucci, S. Ransom, M. Roberts, and J. Hessels, *Nature (London)* **467**, 1081 (2010).
- [31] E. Fonseca, T. T. Pennucci, J. A. Ellis, I. H. Stairs, D. J. Nice, S. M. Ransom *et al.*, *Astrophys. J.* **832**, 167 (2016).
- [32] Z. Arzoumanian, A. Brazier, S. Burke-Spolaor, S. Chamberlin, S. Chatterjee, B. Christy *et al.*, *Astrophys. J. Suppl.* **235**, 37 (2018).
- [33] J. Antoniadis, P. C. Freire, N. Wex, T. M. Tauris, R. S. Lynch *et al.*, *Science* **340**, 1233232 (2013).
- [34] H. T. Cromartie, E. Fonseca, S. M. Ransom, P. B. Demorest *et al.*, *Nat. Astron.* **4**, 72 (2019).
- [35] E. Fonseca, H. T. Cromartie, T. T. Pennucci, P. S. Ray, A. Y. Kirichenko, S. M. Ransom *et al.*, *Astrophys. J. Lett.* **915**, L12 (2021).
- [36] M. B. Tsang, J. R. Stone, F. Camera, P. Danielewicz, S. Gandolfi, K. Hebeler, C. J. Horowitz, J. Lee, W. G. Lynch, Z. Kohley, R. Lemmon, P. Moller, T. Murakami, S. Riordan, X. Roca-Maza, F. Sammarruca, A. W. Steiner, I. Vidana, and S. J. Yennello, *Phys. Rev. C* **86**, 015803 (2012).
- [37] J. M. Lattimer and Y. Lim, *Astrophys. J.* **771**, 51 (2013).
- [38] A. W. Steiner and S. Gandolfi, *Phys. Rev. Lett.* **108**, 081102 (2012).
- [39] K. Hebeler, J. M. Lattimer, C. J. Pethick, and A. Schwenk, *Astrophys. J.* **773**, 11 (2013).
- [40] A. W. Steiner, J. M. Lattimer, and E. F. Brown, *Eur. Phys. J. A* **52**, 18 (2016).
- [41] J. M. Lattimer and M. Prakash, *Phys. Rep.* **621**, 127 (2016).
- [42] A. L. Watts, N. Andersson, D. Chakrabarty, M. Feroci, K. Hebeler, G. Israel, F. K. Lamb, M. C. Miller, S. Morsink, F. Ozel, A. Patruno, J. Poutanen, D. Psaltis, A. Schwenk, A. W. Steiner, L. Stella, L. Tolos, and M. van der Klis, *Rev. Mod. Phys.* **88**, 021001 (2016).
- [43] M. C. Miller, F. K. Lamb, A. J. Dittmann, S. Bogdanov, Z. Arzoumanian, K. C. Gendreau *et al.*, *Astrophys. J. Lett.* **887**, L24 (2019).
- [44] T. E. Riley, A. L. Watts, S. Bogdanov, P. S. Ray, R. M. Ludlam, S. Guillot, Z. Arzoumanian *et al.*, *Astrophys. J. Lett.* **887**, L21 (2019).
- [45] F. J. Fattoyev, J. Piekarewicz, and C. J. Horowitz, *Phys. Rev. Lett.* **120**, 172702 (2018).
- [46] E. Annala, T. Gorda, A. Kurkela, and A. Vuorinen, *Phys. Rev. Lett.* **120**, 172703 (2018).
- [47] E. R. Most, L. R. Weih, L. Rezzolla, and J. Schaffner-Bielich, *Phys. Rev. Lett.* **120**, 261103 (2018).
- [48] E. P. Zhou, X. Zhou, and A. Li, *Phys. Rev. D* **97**, 083015 (2018).
- [49] B. P. Abbott, R. Abbott, T. D. Abbott, and F. Acernese, *Phys. Rev. Lett.* **121**, 161101 (2018).
- [50] J. D. Walecka, *Ann. Phys. (NY)* **83**, 491 (1974).
- [51] J. Boguta and A. Bodmer, *Nucl. Phys. A* **292**, 413 (1977).
- [52] B. A. Li and X. Han, *Phys. Lett. B* **727**, 276 (2013).
- [53] R. S. Hayano and T. Hatsuda, *Rev. Mod. Phys.* **82**, 2949 (2010).
- [54] L. W. Chen, C. M. Ko, and B. A. Li, *Phys. Rev. Lett.* **94**, 032701 (2005).
- [55] M. B. Tsang, Y. Zhang, P. Danielewicz, M. Famiano, Z. Li, W. G. Lynch, and A. W. Steiner, *Phys. Rev. Lett.* **102**, 122701 (2009).
- [56] P. Danielewicz, P. Singh, and J. Lee, *Nucl. Phys. A* **958**, 147 (2017).
- [57] J. Estee, W. G. Lynch, C. Y. Tsang, and J. Barney, *Phys. Rev. Lett.* **126**, 162701 (2021).

- [58] B. T. Reed, F. J. Fattoyev, C. J. Horowitz, and J. Piekarewicz, *Phys. Rev. Lett.* **126**, 172503 (2021).
- [59] H. Sotani, K. Nakazato, K. Iida, and K. Oyamatsu, *Mon. Not. R. Astron. Soc.* **428**, L21 (2013).
- [60] Q. Zhao, B. Y. Sun, and W. H. Long, *J. Phys. G: Nucl. Part. Phys.* **42**, 095101 (2015).
- [61] G. Baym, C. Pethick, and P. Sutherland, *Astrophys. J.* **170**, 299 (1971).
- [62] K. Iida and K. Sato, *Astrophys. J.* **477**, 294 (1997).
- [63] R. C. Tolman, *Phys. Rev.* **55**, 364 (1939).
- [64] J. Oppenheimer and G. Volkoff, *Phys. Rev.* **55**, 374 (1939).
- [65] T. E. Riley, A. L. Watts, P. S. Ray, S. Bogdanov, S. Guillot, S. M. Morsink *et al.*, *Astrophys. J. Lett* **918**, L27 (2021).
- [66] M. C. Miller, F. K. Lamb, A. J. Dittmann, S. Bogdanov, Z. Arzoumanian, K. C. Gendreau *et al.*, *Astrophys. J. Lett* **918**, L28 (2021).